

HIGH-IONIZATION FE K EMISSION FROM LUMINOUS INFRARED GALAXIES

K. IWASAWA¹, D.B SANDERS², A.S. EVANS³, J.M. MAZZARELLA⁴, L. ARMUS⁵, AND J.A. SURACE⁵

Accepted for publication in ApJ Letters

ABSTRACT

The Chandra component of the Great Observatories All-Sky LIRG Survey (GOALS) presently contains 44 luminous and ultraluminous infrared galaxies with $\log(L_{\text{IR}}/L_{\odot}) = 11.73\text{--}12.57$. Omitting 15 obvious AGNs, the other galaxies are, on average, underluminous in the 2-10 keV band by 0.7 dex at a given far-infrared luminosity, compared to nearby star-forming galaxies with lower star formation rates. The integrated spectrum of these hard X-ray quiet galaxies shows strong high-ionization Fe K emission (Fe XXV at 6.7 keV), which is incompatible with X-ray binaries as its origin. The X-ray quietness and the Fe K feature could be explained by hot gas produced in a starburst, provided that the accompanying copious emission from high-mass X-ray binaries is somehow suppressed. Alternatively, these galaxies may contain deeply embedded supermassive black holes that power the bulk of their infrared luminosity and only faint photoionized gas is visible, as seen in some ULIRGs with Compton-thick AGN.

Subject headings: galaxies: active — galaxies: starburst — infrared: galaxies — X-rays: galaxies

1. INTRODUCTION

While far-infrared (FIR) luminosity⁶ is often assumed to be a good indicator of the star formation rate (SFR) in extragalactic objects (e.g. Young & Scoville 1991, Kennicutt 1998), it has also been argued that, in the absence of active galactic nuclei (AGN), X-ray emission could trace the SFR as well; this latter assumption is based primarily on the observed correlation between X-ray luminosity (usually in the 2-10 keV energy range) and FIR luminosity initially found for nearby actively star-forming galaxies with SFRs $\sim 3\text{--}30 M_{\odot}\text{yr}^{-1}$ (e.g., Ranalli et al. 2003, Grimm et al. 2003; Gilfanov et al. 2004). This relation appears to extend to objects with higher SFR (up to $100 M_{\odot}\text{yr}^{-1}$) and higher redshift (e.g., Hornschemeier et al. 2005; Persic & Rapphaeli 2007, Lehmer et al. 2008). The hard X-ray emission is generally assumed to have a power-law form and to be predominantly due to the collective emission of high-mass X-ray binaries (HMXBs), which are accreting compact objects (neutron stars or black holes) formed following the death of short-lived massive stars, and therefore expected to have a close relationship to the starburst.

There have been, however, indications that objects with very high computed SFRs, such as ultraluminous infrared galaxies (ULIRGs), might depart from the correlation because they are underluminous in X-rays for their computed SFRs (Persic & Rapphaeli 2007, Barger, Cowie & Wang 2007). Arp 220, the nearest ULIRG, is a prime example, with a 2-10 keV luminosity ~ 1 dex below the general $L_X\text{--}L_{\text{FIR}}$ correlation (see Iwasawa et al. 2005).

A further puzzle comes from its X-ray spectrum, which shows a strong high-ionization Fe K line (mainly Fe XXV, Iwasawa et al. 2005). This latter finding means that Arp 220 is not only X-ray under-luminous, but that the hard X-ray emission is not primarily due to X-ray binaries because of the presence of a high-ionization Fe K line. In nearby star-forming galaxies, Fe XXV is much weaker (e.g., Cappi et al 1999) or undetected, which is consistent that the hard X-ray emission is dominated by HMXBs. These peculiar properties of the nearest ULIRGs clearly warrant further investigation with a larger sample of (U)LIRGs.

The Great Observatory All-sky LIRGs Survey (GOALS)⁷ is a multi-wavelength study of the most luminous infrared-selected galaxies in the local Universe, selected from the flux-limited *IRAS* Revised Bright Galaxy Sample (RBGS: Sanders et al. 2003). An overview of GOALS is given in Armus et al. (2009). C-GOALS (PI: D. B. Sanders) is the X-ray component of the project utilizing data from the Chandra X-ray Observaotry (*Chandra*, hereafter). Details of the X-ray observations are described in Iwasawa et al. in prep. Here we report results focusing primarily on the $L_X\text{--}L_{\text{FIR}}$ relation and the spectral properties of the hard X-ray emission, with special attention to the Fe K band.

The cosmology used to calculate luminosities in this paper is $H_0 = 70 \text{ km s}^{-1} \text{ Mpc}^{-1}$, $\Omega_M = 0.3$, $\Omega_{\Lambda} = 0.7$, based on the latest WMAP results (Hinshaw et al. 2009).

2. THE SAMPLE

The current C-GOALS sample is complete down to $\log(L_{\text{IR}}/L_{\odot}) = 11.73$, and consists of 44 galaxies from the RBGS with redshifts $z = 0.010\text{--}0.088$ (see Table 1). We first removed obvious AGN as follows. The primary criterion was a flat X-ray spectrum, assessed by the X-ray color or hardness ratio (HR). The X-ray color is defined as $HR = (H - S)/(H + S)$, where H is the 2-8 keV counts and S is the 0.5-2 keV counts. Objects

¹ INAF-Osservatorio Astronomico di Bologna, Via Ranzani, 1, 40127 Bologna, Italy

² Institute for Astronomy, 2680 Woodlawn Drive, Honolulu, Hawaii 96822-1839

³ Department of Astronomy, University of Virginia, 530 McCormick Road, Charlottesville, VA 22904 and NRAO, 520 Edgemont Road, Charlottesville, VA 22903-2475

⁴ IPAC, California Institute of Technology, Pasadena, CA 91125

⁵ *Spitzer* Science Center, California Institute of Technology, Pasadena, CA 91125

⁶ $L_{\text{FIR}} \equiv L(40\text{--}400\mu\text{m})$, as determined using the prescription described in Lonsdale et al. (1985)

⁷ More information about GOALS is available at <http://goals.ipac.caltech.edu/>

TABLE 1
THE C-GOALS SAMPLE.

Object	$\log L_{\text{FIR}}/L_{\odot}$	$\log L_{\text{HX}}/\text{erg s}^{-1}$	Object	$\log L_{\text{FIR}}/L_{\odot}$	$\log L_{\text{HX}}/\text{erg s}^{-1}$
HXQ sample					
F17207-0014	12.42	41.34	NGC 3690 E	11.49	41.00
F19297-0406	12.39	41.26	ESO 593-IG8	11.83	41.28
P07251-0248	12.34	< 40.90	VV 705	11.79	40.83
F12112+0305	12.30	41.60	ESO 255-IG7	11.75	41.46
Arp 220	12.22	40.96	F18293-3413	11.76	41.15
F22491-1808	12.18	40.78	F10173+0828	11.76	39.82
F23365+3604	12.11	41.20	ESO 203-IG1	11.84	< 40.48
F10565+2448	11.99	41.20	F01364-1042	11.82	41.18
F15250+3608	11.98	< 40.65	ESO 239-IG2	11.73	40.99
F09111-1007	11.97	41.11	P21101+5810	11.71	40.30
ESO 286-IG19	11.98	41.32	VV 250	11.68	41.49
VII Zw31	11.89	41.43	F10038-3338	11.69	40.80
ESO 69-IG6	11.88	41.18	ESO 77-IG14	11.67	41.15
F17132+5313	11.84	40.93	UGC 4881	11.65	40.73
II Zw96	11.94	41.18	IC 883	11.65	40.81
AGN sample					
Mrk 231	12.37	42.48	P19542+1110	12.06	42.61
F14348-1447	12.35	41.77	ESO 148-IG2	11.95	41.92
P09022-3615	12.24	42.30	UGC 5101	11.93	41.67
P13120-5453	12.24	41.67	NGC 3690 W	11.32	41.00
F14378-3651	12.16	41.53	NGC 6240	11.81	42.54
Mrk 273	12.15	42.40	ESO 60-IG16	11.71	41.86
F05189-2524	12.08	43.11	VV 340a	11.66	41.46
F08572+3915	12.07	41.30			

NOTE. — Source names beginning with "F" or "P" are from the IRAS Faint Source Catalog or Point Source Catalog, respectively. with $HR > -0.3$ are classified as an AGN. This threshold is chosen because ULIRGs known to host AGN (Mrk 231, Mrk 273, UGC 5101) cluster just above this value. All of the optically identified AGN are selected by this criterion. However, Compton-thick AGN are generally missed by this criterion because of their weakness in the hard band. Therefore, objects that show a strong FeK line at 6.4 keV, a characteristic signature of a Compton-thick AGN, are also classified as AGN (NGC 6240, NGC 3690 West, VV 340a). These criteria classify 15 objects as AGN, and they are excluded from further discussion leaving an "hard X-ray quiet" (HXQ, as defined by their small HR) sample of 30 objects (including NGC 3690 East). The SFR of these 30 HXQ galaxies, calculated assuming that their FIR luminosity is due to dust heated by star formation alone, ranges from 60 to 300 $M_{\odot} \text{ yr}^{-1}$.

3. L(2-10 KEV) AND L(FIR) RELATION

The sensitivity of *Chandra* declines steeply above 7 keV. The 2-10 keV luminosity is estimated by extrapolating the spectral model that describes the data up to 7 keV. When multiple hard X-ray sources are present in a single object, those which have no *Spitzer*-MIPS 24 μm counterpart are excluded for calculating the 2-10 keV luminosity, assuming they have no relation with the IRAS measured luminosity. In NGC 3690, the western and eastern galaxies are treated separately due to the difference in classification, and their FIR luminosity ratio is assumed to be 1:2 based on the 38 μm study (Charmandaris et al. 2002). The X-ray luminosity is as observed in the rest-frame 2-10 keV band, corrected only for Galactic absorption. The median value of the 2-10 keV luminosity is $1.4 \times 10^{41} \text{ erg s}^{-1}$ (which also matches the mean).

Figure 1 shows a plot of hard X-ray luminosity, $L(2-10 \text{ keV})$, versus FIR luminosity, $L(40-400 \mu\text{m})$, for our complete sample of 44 RBGS galaxies listed in Table 1.

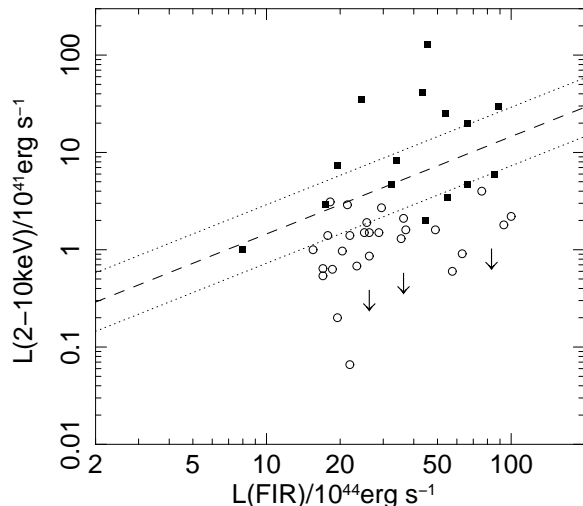


FIG. 1.— $L(2-10 \text{ keV})$ versus $L(\text{FIR})$ for the GOALS AGN (filled squares) and HXQ (open circles) galaxies listed in Table 1. For the three objects with no 2-10 keV detection, the 95 per cent upper limits derived by following Kraft et al. (1991) are shown. The dashed line indicates the correlation for the sample of Ranalli et al. (2003). The dotted lines show a factor of 2 above and below the Ranalli et al. correlation, within which the other studies of the same relationship lie.

For the GOALS HXQ galaxies alone, no clear correlation is seen (Kendal's $\tau \simeq 0.3$) in the limited FIR luminosity range. The correlation obtained by Ranalli et al. (2003) is re-derived in the same way as done for our sample: $\log L(2-10 \text{ keV}) = -3.84 \log L(\text{FIR})$. This is fully consistent with the original relation with an offset due to the wider FIR wavelength range. The L_X -SFR correlations studied by various authors (e.g., Grimm et al. 2003, Perseic & Raphaeli 2007, Lehmer et al. 2008) all lie within a factor of ± 2 of Ranalli et al. (2003) as indicated in the figure. The correlation line is consistent with the upper envelope of the HXQ sample. Most of our HXQ galaxies lie well below this correlation. The median value of the logarithmic ratio of $L(2-10 \text{ keV})$ and $L(\text{FIR})$ is -4.5 , which means our sample of HXQ galaxies is ~ 0.7 dex underluminous in the 2-10 keV band for a given $L(\text{FIR})$, or corresponding SFR. We note that, given the lack of correlation in our sample, this is merely a comparison of the average value relative to the L_X - L_{FIR} correlation.

4. THE INTEGRATED 4-8 KEV SPECTRUM

We investigate the integrated hard-band spectrum of the 30 HXQ galaxies, since they are too faint in hard X-rays to allow an individual inspection for the iron line. Although detection of the FeK line has been reported for the XMM-Newton spectra of NGC 3690 East (Ballo et al. 2004) and Arp 220 (Iwasawa et al. 2005), the line does not have sufficient counts in the Chandra data for a significant detection (see e.g., Clements et al. 2002). These two objects are included in the integrated hard-band spectrum and their contribution to the total spectrum is also investigated. In cases where multiple hard X-ray sources are detected in a single object (IRAS F09111-1007, ESO 255-IG007, VV 250, ESO 77-IG014, IRAS F12112+0305, VV 705, UGC 4881), multiple apertures were selected accordingly.

Given that our primary interest is in the FeK properties, we restrict the analysis to the FeK and neighboring band (4.25-7.65 keV in the rest-frame). The FeK

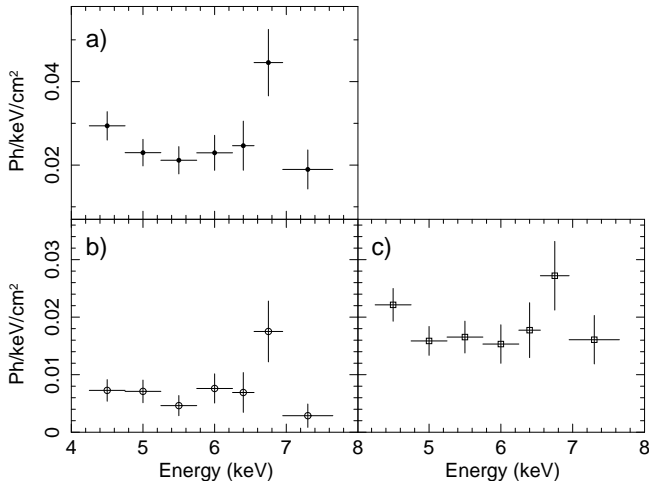


FIG. 2.— (a) The integrated 4.25–7.65 keV spectrum of the 29 HXQ objects in Table 1. The energy is in the rest-frame. An excess in the high-ionization Fe K band (primarily due to Fe XXV) at 6.55–6.95 keV is clearly visible. The continuum is flat ($\Gamma = 1.1 \pm 0.5$) and the Fe K band excess has $EW \sim 1$ keV. (b) The integrated spectrum of Arp 220 and NGC 3690 E, two Fe XXV emitters known from XMM-Newton observations. (c) The integrated spectrum of the HXQ sample excluding Arp 220 and NGC 3690 E. Even without the two known Fe XXV emitters, a comparable excess flux above the continuum in the Fe XXV band is present, indicating that other galaxies make a significant contribution to the total line flux in a).

complex generally consists of two components with distinct ionization states: (a) cold Fe at 6.4 keV; and (b) highly ionized Fe XXV (6.7 keV) with a minor contribution from Fe XXVI (7.0 keV). These two components can be separated well at the spectral resolution of the Chandra ACIS-S. We define two spectral bands centered on the respective line components (6.35–6.55 keV and 6.55–6.95 keV), and five neighboring bands for the continuum, giving seven spectral bands over the range 4.25–7.65 keV in the rest-frame.

The hard X-ray sources of our sample are generally compact, and a small extraction radius, typically ~ 1.5 – $2''$, is used. The detected counts have been corrected for background using the data from a source-free area on the detector in the same observation, although the correction is almost negligible with such a small aperture.

For individual objects, source counts recorded in seven bands corresponding to the pre-defined rest-frame bands were accumulated. The detector response curve was corrected by dividing by the mean effective area of each spectral band. As most sources have only a few counts over the energy range, stacking was done as a straight integration of individual sources, neither normalizing by the exposure time nor source brightness.

The total source counts accumulated in the rest-frame 4.25–7.65 keV band for the HXQ sample are 296 ct. The integrated spectrum is shown in Fig. 2a. A strong Fe K line is immediately recognized with a 3σ excess. The line peaks at the high-ionization Fe K band (6.55–6.95 keV), indicating that the line is primarily due to Fe XXV from a highly ionized medium. The total counts collected in this line band is 35 ct. There might also be a slight excess in the 6.4 keV line band, which is however not significant.

Given the limited statistics, a further analysis beyond the line detection is not warranted. However, given our stacking method, which is biased for sources that are bright and/or with a long exposure, it is at least worth

examining whether Arp 220 and NGC 3690 E, the two known Fe K emitters from their XMM-Newton spectra, dominate the line detection. These two objects and the rest of the HXQ sample were integrated separately, and their spectra are presented in Fig. 2b and 2c. Both spectra show a $\simeq 2\sigma$ excess in the Fe XXV band with comparable line fluxes. This means that, besides Arp 220 and NGC 3690 E, there is a significant contribution by other galaxies to the detected line flux. The higher continuum level in the spectrum of the sample without Arp 220 and NGC 3690 E (Fig. 2c) suggests that some sources without strong Fe K emission are present, and that they may be dominated by HMXBs as found in nearby star-forming galaxies.

Fitting a power-law to the continuum gives a photon index of $\Gamma = 1.1 \pm 0.5$, indicating a rather hard continuum above 4 keV. The equivalent width of the excess in the Fe K band with respect to the power law continuum is $EW = 0.9 \pm 0.3$ keV. The 90% upper limit of the EW for a 6.4 keV line is 120 eV.

Fitting a thermal spectrum (MEKAL) gives a temperature of $kT = 8 \pm 2$ keV and an Fe metallicity consistent with the solar value. Considering that the integrated spectrum is diluted by some sources that contribute only to the continuum emission (see above), the Fe metallicity of the line emitting sources is likely to be super-solar.

Regardless of the choice of spectral model, the strong high-ionization Fe K line is not compatible with the X-ray spectrum of known HMXBs. Fe K emission is often observed from HMXBs in our Galaxy, but the major component is the cold line at 6.4 keV and its EW is on average ~ 200 – 300 eV (e.g. White et al. 1983). The much stronger, high-ionization line in the integrated spectrum of the HXQ sample suggests that X-ray binaries are not the primary source of the 4–8 keV emission.

5. DISCUSSION

The general quietness of hard X-ray emission in the HXQ galaxies (Fig. 1) is likely related to the detection of the high-ionization Fe K feature, which rules out HMXBs as the primary origin of the faint hard X-ray emission.

The powerful FIR emission in the HXQ (U)LIRGs predicts an abundance of HMXBs if star formation is the dominant power source. The Chandra spectra, however, suggests these sources contribute little to the hard X-ray emission. Therefore, either the bulk of the HMXBs are missing or they are heavily obscured from view. Suppose heavy obscuration is the cause. Since the Fe K band is still transparent to $N_{\text{H}} \sim 10^{24}$ cm $^{-2}$, the obscuring column has to be larger, perhaps the order of 10^{25} cm $^{-2}$. A dense, nuclear molecular disk (with a dynamical mass of the order of $10^9 M_{\odot}$) is often found in the central part of ULIRGs (e.g., Bryant & Scoville 1999) and thus, such a large column may not be unrealistic. The size of the nuclear molecular disk is generally found to be a few 100 pc but the densest part can be as small as 30 pc, as found by high-resolution studies of Arp 220 (Downes & Eckart 2007, Sakamoto et al. 2008, Aalto et al. 2009), where a rough estimate of the density is 10^5 – 10^6 cm $^{-3}$. According to Grimm et al. (2003), the number of HMXBs with $L_{\text{X}} > 2 \times 10^{38}$ erg s $^{-1}$, which would dominate the integrated luminosity of the entire HMXB population, is ~ 300 ($SFR/100 M_{\odot} \text{ yr}^{-1}$). For $SFR = 200 M_{\odot} \text{ yr}^{-1}$, as estimated for Arp 220, the number is ~ 600 , and most

of them need to be confined within 30 pc in order for their radiation to be suppressed. The required stellar density is unusually high and could be a problem in this particular case. The other galaxies may have a larger starburst region and could avoid this problem provided the required mass of the obscuring gas does not exceed the dynamical mass.

Once the HMXBs are obscured from view, the Fe XXV spectrum can be explained by high-temperature ($T \sim 10^8$ K), thermal gas produced by a starburst. Possible sources are (i) an internally shocked hot bubble⁸ produced by thermalizing the energy of supernovae (SNe) and stellar winds, as predicted by, e.g., Chevalier & Clegg (1985); and (ii) collective luminous SNe. The latter is ruled out if HMXBs are all embedded in heavy obscuration because the SNe should also be embedded in the same obscuring material. The former would excavate the obscuration and become visible. With the assumed high SFR, the luminosity and the spectrum with strong Fe XXV can be reproduced (e.g., Iwasawa et al. 2005 for Arp 220). The diffuse hard X-ray emission seen in M 82 (Griffiths et al. 2000, Strickland & Heckman 2007, Ranalli et al. 2008), after removing resolved X-ray binaries, has, in fact, a comparable X-ray to FIR ratio with that of our GOALS HXQ sample. The strong Fe line is also well matched with the prediction for metal enriched gas of this origin.

With the presence of dense nuclear gas, a heavily obscured AGN is also a possible explanation for the X-ray spectra of our HXQ sample. Massive black holes in the process of rapid growth are naturally expected to be present in (U)LIRGs. When a central AGN is deeply buried with a covering factor nearly unity, reprocessed light from the obscuring matter would have difficulty escaping. The high-ionization Fe K line could then originate from extended, low density gas which is photoionized by the AGN. In a number of Compton thick Seyfert

2 galaxies, e.g., NGC 1068, Fe XXV has been seen (but normally weaker than the cold line at 6.4 keV). This is in fact the feature originally predicted by Krolik & Kallman (1987) when assuming a likely scattering medium to produce the polarized broad-line region in NGC 1068 (Antonucci & Miller 1985). Where the cold X-ray reflection is suppressed, the weak, highly photoionized gas could be the only observable feature. We note that Fe XXV has been observed as the primary Fe K feature in some Compton-thick AGN residing in the ULIRGs IRAS F00183–7113 (Nandra & Iwasawa 2007, Ruiz et al. 2007), The Superantennae (Braitto et al. 2009), and possibly UGC 5101.

In Arp 220, recent measurements of a compact dust emission source with a steep temperature gradient in the western nucleus provides an argument for an AGN (Downes & Eckart 2007, Aalto et al. 2009; but see Sakamoto et al. 2008). Millimeter wavelength molecular line observations also suggest the presence of X-ray dominated chemistry, which favors heating by AGN (Aalto et al. 2007, Imanishi et al. 2007; e.g., Meijerink & Spaans 2005 for theory). The similarity of the X-ray properties suggests that the same explanation might apply for at least some of the GOALS HXQ galaxies – i.e., despite the lack of outward evidence of an AGN, a significant fraction of the infrared output could be powered by a heavily obscured AGN.

ACKNOWLEDGEMENTS

This research was supported in part by NASA through *Chandra* award Number GO7-8108A, issued by the *Chandra X-Ray Observatory*, which is operated by the Smithsonian Astrophysical Observatory for and on behalf of NASA under contract NAS8-39073. We acknowledge use of the NASA/IPAC Extragalactic Database (NED), and the software packages CIAO and HEASoft.

stellar medium (e.g., Tomisaka & Ikeuchi 1988).

REFERENCES

- Aalto, S., Wilner, D., Spaans, M., Wiedner, M. C., Sakamoto, K., Black, J. H., & Caldas, M. 2009, *A&A*, 493, 481
- Antonucci, R. R. J., & Miller, J. S. 1985, *ApJ*, 297, 621
- Armus, L., et al., 2009, *PASP*, submitted
- Ballo, L., Braitto, V., Della Ceca, R., Maraschi, L., Tavecchio, F., & Dadina, M. 2004, *ApJ*, 600, 634
- Barger, A. J., Cowie, L. L., & Wang, W.-H. 2007, *ApJ*, 654, 764
- Bryant, P. M., & Scoville, N. Z. 1999, *AJ*, 117, 2632
- Cappi, M., et al. 1999, *A&A*, 350, 777
- Charmandaris, V., Stacey, G. J., & Gull, G. 2002, *ApJ*, 571, 282
- Chevalier, R. A., & Clegg, A. W. 1985, *Nature*, 317, 44
- Clements, D. L., McDowell, J. C., Shaked, S., Baker, A. C., Borne, K., Colina, L., Lamb, S. A., & Mundell, C. 2002, *ApJ*, 581, 974
- Downes, D., & Eckart, A. 2007, *A&A*, 468, L57
- Gilfanov, M., Grimm, H.-J., & Sunyaev, R. 2004, *MNRAS*, 347, L57
- Griffiths, R. E., Ptak, A., Feigelson, E. D., Garmire, G., Townsley, L., Brandt, W. N., Sambruna, R., & Bregman, J. N. 2000, *Science*, 290, 1325
- Grimm, H.-J., Gilfanov, M., & Sunyaev, R. 2003, *MNRAS*, 339, 793
- Hinshaw, G., et al. 2009, *ApJS*, 180, 225
- Hornschemeier, A. E., Heckman, T. M., Ptak, A. F., Tremonti, C. A., & Colbert, E. J. M. 2005, *AJ*, 129, 86
- Imanishi, M., Nakanishi, K., Tamura, Y., Oi, N., & Kohno, K. 2007, *AJ*, 134, 2366
- Iwasawa, K., Sanders, D. B., Evans, A. S., Trentham, N., Miniutti, G., & Spoon, H. W. W. 2005, *MNRAS*, 357, 565
- Kennicutt, R. C., Jr. 1998, *ARA&A*, 36, 189
- Kraft, R. P., Burrows, D. N., & Nousek, J. A. 1991, *ApJ*, 374, 344
- Krolik, J. H., & Kallman, T. R. 1987, *ApJ*, 320, L5
- Lehmer, B. D., et al. 2008, *ApJ*, 681, 1163
- Lonsdale, C. J., Helou, G., Good, J. C., & Rice, W. L. 1985, *Cataloged Galaxies and Quasars Detected in the IRAS Survey (JPL D-1932)* (Pasadena: JPL)
- Meijerink, R., & Spaans, M. 2005, *A&A*, 436, 397
- Nandra, K., & Iwasawa, K. 2007, *MNRAS*, 382, L1
- Persic, M., & Rephaeli, Y. 2007, *A&A*, 463, 481
- Ranalli, P., Comastri, A., Origlia, L., & Maiolino, R. 2008, *MNRAS*, 386, 1464
- Ranalli, P., Comastri, A., & Setti, G. 2003, *A&A*, 399, 39
- Ruiz, A., Carrera, F. J., & Panessa, F. 2007, *A&A*, 471, 775
- Sakamoto, K., et al. 2008, *ApJ*, 684, 957
- Sanders, D. B., Mazzarella, J. M., Kim, D.-C., Surace, J. A., & Soifer, B. T. 2003, *AJ*, 126, 1607
- Scoville, N. Z., Yun, M. S., & Bryant, P. M. 1997, *ApJ*, 484, 702
- Strickland, D. K., & Heckman, T. M. 2007, *ApJ*, 658, 258
- Tomisaka, K., & Ikeuchi, S. 1988, *ApJ*, 330, 695
- White, N. E., Swank, J. H., & Holt, S. S. 1983, *ApJ*, 270, 711
- Young, J. S., & Scoville, N. Z. 1998, *ARA&A*, 29, 581